

Multilayer cuprate superconductors as possible systems described by resonating-valence-bond and antiferromagnetic orders

Hiroyuki Yamase¹, Masanao Yoneya², and Kazuhiro Kuboki²

¹ *National Institute for Materials Science, Tsukuba 305-0047, Japan*

² *Department of Physics, Kobe University, Kobe 657-8501, Japan*

(Dated: November 6, 2018)

Abstract

Coexistence of antiferromagnetism and d -wave superconductivity within a CuO_2 plane was recently observed in a wide doping region for multilayer high-temperature cuprate superconductors. We find that the experimental phase diagram is well reproduced in the slave-boson mean-field scheme of the two-dimensional t - J model by including antiferromagnetic order. We argue that weak three dimensionality coming from a multilayer structure is sufficient to stabilize antiferromagnetic order and its coexistence with superconductivity.

PACS numbers: 74.20.Mn, 74.72.-h, 74.25.Ha, 71.10.Fd

I. INTRODUCTION

High-temperature superconductivity (SC) is one of the most fascinating topics in physics. The discovery of the magnesium diboride in 2001 (Ref. 1) immediately generated very intensive studies. The recent discovery of ferropnictides² also attracts tremendous attention, opening a new branch in condensed matter physics. It is however still only cuprate superconductors especially multilayer cuprates such as $\text{HgBa}_2\text{Ca}_{n-1}\text{Cu}_n\text{O}_y$ and $\text{TlBa}_2\text{Ca}_{n-1}\text{Cu}_n\text{O}_y$ with $n \geq 3$ that achieve superconducting transition temperature (T_c) more than 100 K (Ref. 3); we mean by "multilayer" three or more layers in a unit cell in this paper. For such multilayer cuprates, the previous theoretical studies⁴⁻⁶ paid attention to the description of a superconducting phase coherence between the layers, including a possible charge imbalance between the layers in a unit cell. In those studies there was a tacit assumption that the property of each CuO_2 plane is essentially the same as that in single- and bi-layer cuprates in the sense that AF is realized for very low doping and is replaced by SC for moderate doping without the coexistence with AF within a CuO_2 plane.

However, the recent NMR measurements for multilayer cuprate superconductors⁷⁻⁹ revealed the phenomena very different from those in single- and bi-layer cuprates: antiferromagnetism (AF) in the Mott insulator survives up to rather high carrier doping and coexists with a superconducting state. The coexistence was due to not a proximity effect between the layers, but a phase transition within a CuO_2 plane at low temperatures.

This observation sharply contrasts with a widely accepted viewpoint that AF in the Mott insulator is rapidly suppressed by a tiny amount of carrier doping and the d -wave superconducting state is instead stabilized in a wide doping region, typically in 5 – 30%. The latter viewpoint is based on the data for single- and bi-layer cuprates such as La- and Y-based compounds, for which a huge number of studies have been performed last about 25 years in a systematic way. Compared with those materials, multilayer cuprates are much less investigated. They contain completely flat CuO_2 planes with a perfect square lattice and are known to be free from disorder, in contrast to La- and Y-based cuprates. They also achieve higher T_c than that for single- and bi-layer cuprates.³ In this sense multilayer cuprates can be viewed as an ideal system to study the mechanism of high T_c . Nonetheless, the basic theoretical framework for multilayer cuprates has not been identified so far.

Moreover the origin of the pseudogap¹⁰ is still a central issue on high-temperature SC

and a clue to resolve it is highly desired. Therefore it is of great importance to shed light on an issue of the pseudogap in multilayer cuprates from a theoretical point of view, which may in turn provide a crucial insight into the pseudogap in single- and bi-layer cuprates.

In this paper, we explore the basic theoretical framework which captures the essential features recently reported for the multilayer cuprates.⁷⁻⁹ We invoke Anderson's resonating-valence-bond (RVB) scenario,¹¹ that is, the undoped CuO_2 plane is assumed to be in the RVB spin liquid state and the preexisting spin singlet pairs can become charged superconducting pairs once they are mobile by carrier doping. This idea was well described in terms of the two-dimensional (2D) t - J model. In particular, the slave-boson mean-field theory^{12,13} and the gauge theory,¹⁴ which takes low-energy fluctuations around the mean-fields into account, turned out to capture many important properties of single- and bi-layer cuprate superconductors.¹⁵⁻¹⁷

In the standard RVB framework, AF is assumed to be strongly fluctuating, not to be ordered. However, antiferromagnetic order can be easily stabilized in the presence of weak three dimensionality coming from a multilayer structure. This effect can be incorporated phenomenologically by including AF as a possible mean-field order parameter within a single-layer model. Such a calculation was performed in the slave-boson mean-field scheme^{18,19} and variational Monte Carlo^{20,21} for the 2D t - J model in a different context, showing that AF extends to a high doping rate and coexists with SC. However, the coexistence obtained previously was found to be substantially suppressed by the presence of a long-range hopping amplitude, leading to a pure antiferromagnetic state.^{19,21} Moreover, the previous theoretical results^{18,19} typically exhibited reentrant behavior of the critical temperature of AF at low temperatures, which was not observed experimentally.⁷

We perform the slave-boson mean-field analysis of the t - J model by including antiferromagnetic order. While we analyze the 2D model and do not take multilayer degrees of freedom into account, we consider that a special feature of multilayer cuprates is included phenomenologically by allowing AF order as a possible mean field in our analysis. In this framework, important features of the phase diagram for multilayer cuprates are obtained.²² We argue that the essential difference between multilayer cuprates and single- and bi-layer cuprates lies in the presence of weak three dimensionality and thus the phase diagram of the former is well described by both RVB and AF, while that of the latter is simply by the RVB as already investigated. In contrast to single- and bi-layer cuprates, the pseudogap may be

substantially diminished in the heavily underdoped region of multilayer cuprates.

II. MODEL AND FORMALISM

We employ the 2D t - J model on a square lattice

$$\mathcal{H} = - \sum_{i,j,\sigma} t_{ij} \tilde{c}_{i\sigma}^\dagger \tilde{c}_{j\sigma} + J \sum_{\langle i,j \rangle} \mathbf{S}_i \cdot \mathbf{S}_j, \quad (1)$$

where the transfer integrals t_{ij} are finite for the first- (t), second- (t'), and third-nearest neighbor bonds (t''), and vanish otherwise. $J(> 0)$ is the antiferromagnetic superexchange interaction and $\langle i,j \rangle$ denotes the nearest neighbor bonds. $\tilde{c}_{i\sigma}$ is the electron operator in the Fock space without double occupancy and we treat this condition using the slave-boson method²³ by writing $\tilde{c}_{i\sigma} = b_i^\dagger f_{i\sigma}$ under the local constraint $\sum_\sigma f_{i\sigma}^\dagger f_{i\sigma} + b_i^\dagger b_i = 1$ at every i site. Here $f_{i\sigma}$ (b_i) is a fermion (boson) operator that carries spin σ (charge e); the fermions (bosons) are frequently referred to as spinons (holons). The spin operator is expressed as $\mathbf{S}_i = \frac{1}{2} \sum_{\alpha\beta} f_{i\alpha}^\dagger \boldsymbol{\sigma}_{\alpha\beta} f_{i\beta}$ with $\boldsymbol{\sigma}$ being the Pauli matrices.

Hamiltonian (1) is decoupled by introducing the following order parameters:^{18,19} the staggered magnetization $m = \frac{1}{2} \langle f_{i\uparrow}^\dagger f_{i\uparrow} - f_{i\downarrow}^\dagger f_{i\downarrow} \rangle e^{i\mathbf{Q}\cdot\mathbf{r}_i}$ with $\mathbf{Q} \equiv (\pi, \pi)$; the bond order parameter for spinons and holons, $\langle \sum_\sigma f_{i\sigma}^\dagger f_{j\sigma} \rangle$, $\langle b_i^\dagger b_j \rangle$; we denote $\chi = \langle \sum_\sigma f_{i\sigma}^\dagger f_{j\sigma} \rangle$ for the nearest neighbor bond; the singlet RVB pairing $\Delta_\tau = \langle f_{i\uparrow}^\dagger f_{i+\tau\downarrow} - f_{i\downarrow}^\dagger f_{i+\tau\uparrow} \rangle$ with $\tau = x, y$. Here we assume that all these expectation values are real and independent of i . We can show that the $d_{x^2-y^2}$ -wave pairing state is the most stable, i.e., $\Delta_x = -\Delta_y \equiv \Delta_0$. Although the bosons are not condensed in the present mean-field scheme at finite temperature (T), they are almost condensed at low T and for finite carrier doping $\delta (\gtrsim 0.02)$.¹⁸ Hence we approximate $\langle b \rangle \approx \sqrt{\delta}$ and $\langle b_i^\dagger b_j \rangle \approx \delta$. In principle, the so-called π -triplet pairing state can emerge for a state with $m \neq 0$ and $\Delta_0 \neq 0$,²⁴ but turns out not to be stable in our model. Hence the free energy per lattice site is computed as

$$F = -\frac{2T}{N} \sum_{\mathbf{k}}' \left[\log \left(2 \cosh \frac{\lambda_{\mathbf{k}}^+}{2T} \right) + \log \left(2 \cosh \frac{\lambda_{\mathbf{k}}^-}{2T} \right) \right] + \frac{3J}{4} (\chi^2 + \Delta_0^2) + 2Jm^2 - \mu\delta, \quad (2)$$

where $\lambda_{\mathbf{k}}^\pm = \sqrt{(\eta_{\mathbf{k}}^\pm)^2 + \Delta_{\mathbf{k}}^2}$ is the spinon's band dispersion in the presence of m and Δ_0 ; $\eta_{\mathbf{k}}^\pm = \xi_{\mathbf{k}}^+ \pm D_{\mathbf{k}}$, $D_{\mathbf{k}} = \sqrt{(\xi_{\mathbf{k}}^-)^2 + (2Jm)^2}$, $\xi_{\mathbf{k}}^\pm = (\xi_{\mathbf{k}} \pm \xi_{\mathbf{k}+\mathbf{Q}})/2$, $\xi_{\mathbf{k}} = -2(t\delta + \frac{3}{8}J\chi)(\cos k_x + \cos k_y) - 4t'\delta \cos k_x \cos k_y - 2t''\delta(\cos 2k_x + \cos 2k_y)$, and $\Delta_{\mathbf{k}} = -\frac{3}{4}J\Delta_0(\cos k_x - \cos k_y)$; μ and

N denote the chemical potential and the total number of lattice sites, respectively; the sum of momentum is taken over the magnetic Brillouin zone $|k_x| + |k_y| \leq \pi$.

Because we relax the local constraint to a global one $\langle \sum_{\sigma} f_{i\sigma}^{\dagger} f_{i\sigma} \rangle = 1 - \delta$ and $\langle b_i^{\dagger} b_i \rangle = \delta$ in the present mean-field theory, our approximation may be reliable as long as electrons are in coherent motion. In the present case, since χ tends to saturate for $\delta \gtrsim 0.05$ [Fig. 1(b)], we expect that our approximation is sufficiently reliable in such a region, where most of experimental data have been obtained so far.

To examine a possibility of the incommensurate antiferromagnetic instability, we also compute the longitudinal magnetic susceptibility $\chi(\mathbf{q})$ in the random phase approximation: $\chi(\mathbf{q})^{-1} = \chi_0(\mathbf{q})^{-1} + 2J(\cos q_x + \cos q_y)$ and

$$\chi_0(\mathbf{q}) = \frac{1}{4N} \sum_{\mathbf{k}} \left[C_{\mathbf{k}, \mathbf{k}+\mathbf{q}}^+ \frac{\tanh \frac{E_{\mathbf{k}}}{2T} - \tanh \frac{E_{\mathbf{k}+\mathbf{q}}}{2T}}{E_{\mathbf{k}} - E_{\mathbf{k}+\mathbf{q}}} + C_{\mathbf{k}, \mathbf{k}+\mathbf{q}}^- \frac{\tanh \frac{E_{\mathbf{k}}}{2T} + \tanh \frac{E_{\mathbf{k}+\mathbf{q}}}{2T}}{E_{\mathbf{k}} + E_{\mathbf{k}+\mathbf{q}}} \right], \quad (3)$$

$$C_{\mathbf{k}, \mathbf{k}+\mathbf{q}}^{\pm} = \frac{1}{2} \left(1 \pm \frac{\xi_{\mathbf{k}} \xi_{\mathbf{k}+\mathbf{q}} + \Delta_{\mathbf{k}} \Delta_{\mathbf{k}+\mathbf{q}}}{E_{\mathbf{k}} E_{\mathbf{k}+\mathbf{q}}} \right). \quad (4)$$

Here $E_{\mathbf{k}} = \sqrt{\xi_{\mathbf{k}}^2 + \Delta_{\mathbf{k}}^2}$ is the spinon's band dispersion for $m = 0$ and the sum of \mathbf{k} is taken over the region $|k_x|, |k_y| \leq \pi$.

The material dependence of cuprate superconductors can be taken into account mainly by different choices of t' and t'' .^{25–28} Hence it is naturally expected that we could invoke specific values of t' and t'' appropriate for multilayer cuprates. This could be achieved for a realistic multilayer model, which also contains other parameters such as interlayer hopping integrals, interlayer exchange interactions, and site potential yielding a charge imbalance between the layers in a unit cell. Given that there is much ambiguity about those parameters and that a special feature of multilayer cuprates is considered phenomenologically in the present analysis by invoking AF order as a possible mean field, we consider the values of t' and t'' simply as phenomenological parameters to reproduce various types of the phase diagram.

III. RESULTS

We determine the mean fields by minimizing the free energy Eq. (2) and obtain the phase diagram in the plane of δ and T . The result for $t/J = 4$, $t'/t = 0.12$, and $t''/t = -0.06$, for which an electron-like Fermi surface is realized in a normal state [Fig. 1(c)], is shown in Fig. 1(a). The temperature T_N denotes the onset of AF, and $T_{\text{RVB}}^{\text{AF}}$ (T_{RVB} and $T_{\text{RVB}}^{\text{noAF}}$)

the onset of singlet pairing in the presence (absence) of AF. At $\delta = 0$, AF is realized and no singlet pairing coexists. With carrier doping, the critical temperature of AF gradually decreases and survives in a wide doping region up to $\delta_N \approx 0.17$; the δ_N is the critical doping rate of AF at $T = 0$. AF suppresses the formation of singlet pairing ($T_{\text{RVB}}^{\text{AF}} < T_{\text{RVB}}^{\text{no AF}}$), but the coexistence is realized at low temperatures. Singlet pairing extends over a wider doping region than AF, and a pure d -wave singlet pairing state is realized at high doping rates. The right-hand panel in Fig. 1(a) magnifies the region around the tetracritical point $(\delta_{\text{tet}}, T_{\text{tet}}) \approx (0.165, 0.031J)$, where the four states, AF, SC, their coexistence, and the normal states, become identical. The order parameters m , Δ_0 , and χ are shown in Fig. 1(b) as a function of δ at low T . Although Δ_0 still increases with decreasing δ in a certain region in $\delta \lesssim \delta_N$, we see that Δ_0 is typically suppressed by the presence of AF compared with Δ_0 for $m = 0$. Similarly the magnitude of χ is suppressed by the presence of m and becomes zero at $\delta = 0$. The system becomes an antiferromagnetic insulator at $\delta = 0$.

A crucial feature of Fig. 1 (a) (see the top right-hand panel) is that in spite of competition of AF and singlet pairing, AF extends to a higher doping region beyond the tetracritical point in the singlet pairing state. This is the crucial difference from the previous work^{18,19} where T_N exhibits reentrant behavior at low T , leading to $\delta_N < \delta_{\text{tet}}$. The difference comes from our careful choice of the band parameters under the constraint $t'' = -t'/2$ (Ref. 29) such that the shape of the Fermi surface around $\delta = \delta_{\text{tet}}$ fulfills the nesting condition of $\mathbf{q} = \mathbf{Q}$ close to the nodal region of the d -wave pairing gap. Hence, the resulting static spin susceptibility $\chi(\mathbf{q})$ shows a maximum at $\mathbf{q} = \mathbf{Q}$ and is not suppressed by the onset of singlet pairing, leading to $\delta_N > \delta_{\text{tet}}$.

The careful choice of the band parameters is not a unique way to obtain a phase diagram similar to Fig. 1(a) when we allow other magnetic orders with $\mathbf{q} \neq \mathbf{Q}$. In Fig. 2(a), we show a representative result. We first minimize the free energy Eq. (2) with respect to the mean fields χ , m , and Δ_0 . We then obtain the lines of T_N , $T_{\text{RVB}}^{\text{AF}}$, and T_{RVB} . The T_N exhibits reentrant behavior around $\delta = \delta_N \approx 0.15$ at low temperatures, in contrast to Fig. 1(a). To investigate a possibility of other magnetic orders, we check a wave vector at which $\chi(\mathbf{q})$ diverges. It turns out that a part of the line T_N [solid line with crosses in Fig. 2(a)] is preempted by the onset of incommensurate antiferromagnetic order T_N^{IC} , where $\chi(\mathbf{q})$ diverges at $\mathbf{q} \neq \mathbf{Q}$. The ordering wave vector \mathbf{q} depends strongly on δ and T . The most crucial point in Fig. 2(a) is that the original reentrant behavior of T_N (solid line with

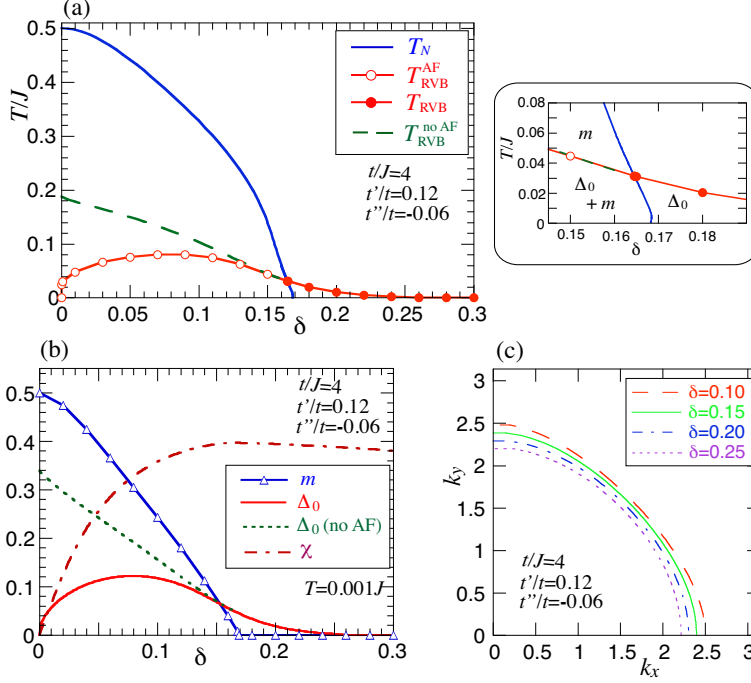


FIG. 1: (Color online) (a) Phase diagram in the plane of δ and T for $t/J = 4$, $t'/t = 0.12$ and $t''/t = -0.06$. T_N is the onset temperature of AF, and $T_{\text{RVB}}^{\text{AF}}$ (T_{RVB} and $T_{\text{RVB}}^{\text{no AF}}$) is that of singlet pairing in the presence (absence) of AF. The right-hand panel magnifies the region around the tetracritical point; the antiferromagnetic and superconducting states are denoted by “ m ” and “ Δ_0 ”, respectively, and their coexistence is by “ $\Delta_0 + m$ ”. (b) δ dependence of the order parameters at $T = 0.001J$. (c) Fermi surfaces in the normal state for several choices of δ .

crosses) is fictitious and instead a true phase boundary is given by T_N^{IC} . We find that these results are generic and applicable for various band parameters, which reproduce an electron-like Fermi surface that does not cross the magnetic Brillouin-zone boundary $|k_x| + |k_y| = \pi$ around $\delta = \delta_{\text{tet}}$ [see Fig. 2(b)]. In this sense, the phase diagram of Fig. 1(a), where AF with $\mathbf{q} = \mathbf{Q}$ is stabilized, should be regarded as a special case requiring a tuning of band parameters as already mentioned above. In fact, if we change the value of t/J in Fig. 1 to $t/J = 3$, keeping t'/t and t''/t unchanged, the Fermi surface stays almost the same, but δ_{tet} shifts to be a bit larger. Such a small shift is sufficient to degrade the nesting condition of $\mathbf{q} = \mathbf{Q}$ around $\delta = \delta_{\text{tet}}$. The resulting T_N exhibits reentrant behavior, which is however preempted by T_N^{IC} , similar to Fig. 2(a). There would also be a possibility that the reentrant behavior of T_N shown in Fig. 2(a) could be preempted by a first order transition to AF with

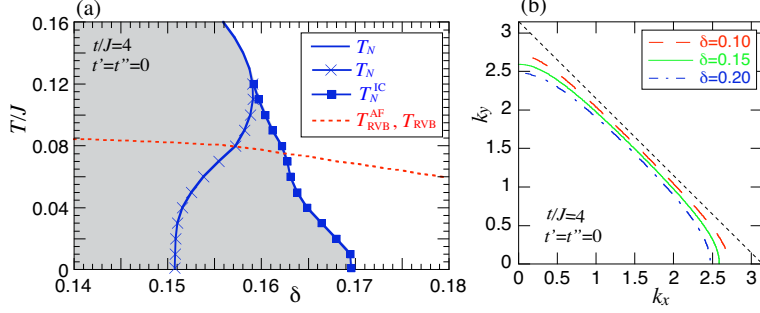


FIG. 2: (Color online) (a) Phase diagram in the plane of δ and T for $t/J = 4$, $t' = t'' = 0$. T_N^{IC} is the onset temperature of incommensurate AF; other notations follow those in Fig. 1(a). AF is realized in the shaded region. (b) Fermi surfaces. The boundary of the magnetic Brillouin zone is denoted by a dotted line.

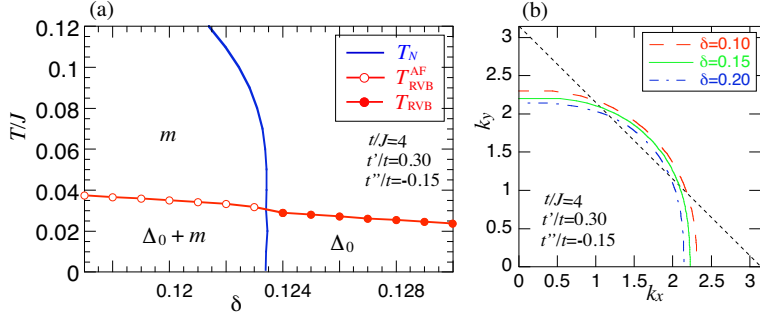


FIG. 3: (Color online) (a) Phase diagram in the plane of δ and T for $t/J = 4$, $t'/t = 0.3$, and $t''/t = -0.15$. The notations follow those in Fig. 1(a). (b) Fermi surfaces. The boundary of the magnetic Brillouin zone is denoted by a dotted line.

$\mathbf{q} = \mathbf{Q}$. However we checked that such a possibility does not occur by observing that the Landau free energy features a single minimum as a function of m .

If an electron-like Fermi surface crosses the magnetic Brillouin-zone boundary around $\delta = \delta_{\text{tet}}$ as shown in Fig. 3(b), which may be applicable to electron-doped cuprates,^{30,31} T_N tends to exhibit a straight line but still features a continuous phase transition [Fig. 3(a)]. Incommensurate magnetic order is not found to be stabilized. On the other hand, for band parameters leading to a hole-like Fermi surface such as that frequently used theoretically for Y- and Bi-based cuprates, AF with $\mathbf{q} = \mathbf{Q}$ is the most stable around δ_N and the line of T_N exhibits reentrant behavior as already seen in the literature.¹⁹

IV. DISCUSSION AND CONCLUSION

Our obtained phase diagrams Figs. 1 and 2 show good agreement with the experimental phase diagram.^{7,9} AF extends over a wide doping region and coexists with SC at low T . Not only the value of δ_N but also the magnitude of m is comparable with the experimental results.⁷⁻⁹ We have invoked an electron-like Fermi surface such as that shown in Figs. 1(c) and 2(b). We expect such a Fermi surface is stabilized as one of Fermi surfaces in multilayer cuprates³² by virtue of strong hybridization between the layers with the dispersion $\epsilon_{\mathbf{k}}^z \propto (\cos k_x - \cos k_y)^2$ (Ref. 29). The angle-resolved photoemission spectroscopy (ARPES) was performed for $\text{Bi}_2\text{Sr}_2\text{Ca}_2\text{Cu}_3\text{O}_{10+y}$ ³³ and $\text{Ba}_2\text{Ca}_3\text{Cu}_4\text{O}_8\text{F}_2$,³⁴ and failed to reveal all Fermi surfaces. In connection with the NMR experiments,⁷⁻⁹ it is desirable to perform the ARPES for Hg- and Tl-based cuprates and to test a possible presence of an electron-like Fermi surface. It is not clear which phase diagram, Fig. 1(a) or Fig. 2(a), is more appropriate to multilayer cuprates, since the NMR does not directly discriminate different ordering patterns of magnetism. Hence it is also desirable to perform neutron scattering measurements for the multilayer cuprates to reveal the wave vector of magnetic order.

The singlet pairing formation of spinons is interpreted as the pseudogap in the slave-boson formalism in the underdoped region. Since the optimal carrier density δ_{op} of multilayer cuprates is situated above the tetracritical point δ_{tet} , T_{RVB} in $\delta_{\text{tet}} \lesssim \delta \lesssim \delta_{\text{op}}$ in the phase diagram is interpreted as the pseudogap temperature T^* . The previous NMR measurements^{35,36} indeed observed the pseudogap behavior of $(T_1 T)^{-1}$ in such a doping region. Since J is around 100-150 meV, the obtained value of T_{RVB} in Figs. 1 and 2 is small compared with the experimental observation.^{35,36} This discrepancy should be explored by including explicitly the multilayer degree of freedom in the present analysis.

On the other hand, for $\delta < \delta_{\text{tet}}$, U(1) gauge fluctuations emerging in the slave-boson formalism are expected to be strongly suppressed in the antiferromagnetic state and thus spinons and holons tend to confine there.³⁷ Therefore we expect that the pseudogap in the antiferromagnetic state is substantially diminished for $\delta < \delta_{\text{tet}}$ and instead the coexistence of AF and SC is realized unless the tendency of carrier localization appears at low temperatures. Around the tetracritical point it is interesting to clarify both theoretically and experimentally how the onset temperature of the pseudogap changes to that of the phase transition to the coexistence with decreasing δ .

A crucial difference between single-layer and multilayer cuprates lies in the difference of antiferromagnetic fluctuations. AF is realized through breaking of continuous symmetry, which thus does not occur at a finite T in a pure 2D system.³⁸ Hence the presence of AF in layered materials is interpreted as coming from weak three dimensionality, which is always present in real systems and in general suppresses fluctuations. In single-layer cuprates, because of the intrinsic low dimensionality due to a tiny coupling between CuO_2 layers along the c axis, antiferromagnetic fluctuations are expected to be so strong that the magnetism is realized only close to the Mott insulator. Moreover some extrinsic effect such as randomness may easily hinder long-range antiferromagnetic order. The standard slave-boson formalism of the t - J model (without AF) was proposed for such cuprate superconductors.¹⁵ On the other hand, for multilayer cuprates, many layers are already present within a unit cell, yielding relatively strong three dimensionality compared with single-layer systems. In addition, each CuO_2 plane is perfectly flat and free from disorder. These can be the main reasons why the present slave-boson mean-field analysis with AF captures essential features observed in multilayer cuprates.⁷⁻⁹ A natural consequence is that AF would extend over a wider doping region by increasing the number of CuO_2 planes in a unit cell unless the value of t/J varies significantly. This tendency is actually reported in Ref. 8.

Multilayer cuprate superconductors achieve much higher T_c than single-layer systems. Hence the understanding of multilayer cuprates is crucially important to elucidate the mechanism of high-temperature SC. We have argued that weak three dimensionality coming from a multilayer structure is sufficient to stabilize AF and that multilayer cuprates can be systems described by RVB and AF in the t - J model, suggesting the importance of the local antiferromagnetic coupling J .

Acknowledgments

We are grateful to H. Mukuda for useful discussions. H.Y. thanks O. K. Andersen, M. Fujita, V. Hinkov, A. A. Katanin, W. Metzner, and R. Zeyher for valuable discussions.

¹ J. Nagamatsu, N. Nakagawa, T. Muranaka, Y. Zenitani, and, J. Akimitsu, Nature **410**, 63 (2001).

- ² Y. Kamihara, T. Watanabe, M. Hirano, and H. Hosono, *J. Am. Chem. Soc.* **130**, 3296 (2008).
- ³ A. Iyo, Y. Tanaka, H. Kito, Y. Kodama, P. M. Shirage, D. D. Shivagan, H. Matsuhata, K. Tokiwa, and T. Watanabe, *J. Phys. Soc. Jpn.* **76**, 094711 (2007).
- ⁴ S. Chakravarty, H.-Y. Kee, and K. Völker, *Nature* **428**, 53 (2004).
- ⁵ T. A. Zaleski and T. K. Kopeć, *Phys. Rev. B* **71**, 014519 (2005).
- ⁶ M. Mori and S. Maekawa, *Phys. Rev. Lett.* **94**, 137003 (2005).
- ⁷ H. Mukuda, Y. Yamaguchi, S. Shimizu, Y. Kitaoka, P. Shirage, and A. Iyo, *J. Phys. Soc. Jpn.* **77**, 124706 (2008).
- ⁸ S. Shimizu, T. Sakaguchi, H. Mukuda, Y. Kitaoka, P. M. Shirage, Y. Kodama, and A. Iyo, *Phys. Rev. B* **79**, 064505 (2009).
- ⁹ S. Shimizu, H. Mukuda, Y. Kitaoka, H. Kito, Y. Kodama, P. M. Shirage, and A. Iyo, *J. Phys. Soc. Jpn.* **78**, 064705 (2009).
- ¹⁰ T. Timusk and B. Statt, *Rep. Prog. Phys.* **62**, 61 (1999).
- ¹¹ P. W. Anderson, *Science* **235**, 1196 (1987).
- ¹² G. Kotliar and J. Liu, *Phys. Rev. Lett.* **38**, 5142 (1988).
- ¹³ Y. Suzumura, Y. Hasegawa, and H. Fukuyama, *J. Phys. Soc. Jpn.* **57**, 2768 (1988).
- ¹⁴ N. Nagaosa and P. A. Lee, *Phys. Rev. Lett.* **64**, 2450 (1990).
- ¹⁵ P. A. Lee, N. Nagaosa, and X.-G. Wen, *Rev. Mod. Phys.* **78**, 17 (2006).
- ¹⁶ H. Yamase and W. Metzner, *Phys. Rev. B* **73**, 214517 (2006); H. Yamase, *ibid* **75**, 014514 (2007).
- ¹⁷ M. Ogata and H. Fukuyama, *Rep. Prog. Phys.* **71**, 036501 (2008).
- ¹⁸ M. Inaba, H. Matsukawa, M. Saitoh, and H. Fukuyama, *Physica C* **257**, 299 (1996).
- ¹⁹ H. Yamase and H. Kohno, *Phys. Rev. B* **69**, 104526 (2004).
- ²⁰ A. Himeda and M. Ogata, *Phys. Rev. B* **60**, R9935 (1999).
- ²¹ C. T. Shih, Y. C. Chen, C. P. Chou, and T. K. Lee, *Phys. Rev. B* **70**, 220502(R) (2004).
- ²² A part of the present work was published as conference proceedings, K. Kuboki, M. Yoneya, and H. Yamase, *Physica C* **470**, S163 (2010).
- ²³ Z. Zou and P. W. Andersen, *Phys. Rev. B* **37**, 627 (1988).
- ²⁴ G. C. Psaltakis and E. W. Fenton, *J. Phys. C* **16**, 3913 (1983).
- ²⁵ T. Tanamoto, H. Kohno, and H. Fukuyama, *J. Phys. Soc. Jpn.* **62**, 717 (1993).
- ²⁶ L. F. Feiner, J. H. Jefferson, and R. Raimondi, *Phys. Rev. Lett.* **76**, 4939 (1996).

- ²⁷ T. Tohyama and S. Maekawa, *Supercond. Sci. Technol.* **13**, R17 (2000).
- ²⁸ E. Pavarini, I. Dasgupta, T. Saha-Dasgupta, O. Jepsen, and O. K. Andersen, *Phys. Rev. Lett.* **87**, 47003 (2001).
- ²⁹ O. K. Andersen, A. I. Lichtenstein, O. Jepsen, and F. Paulsen, *J. Phys. Chem. Solids* **56**, 1573 (1995).
- ³⁰ D. M. King *et al.*, *Phys. Rev. Lett.* **70**, 3159 (1993).
- ³¹ N. P. Armitage *et al.*, *Phys. Rev. Lett.* **88**, 257001 (2002).
- ³² M. Mori, T. Tohyama, and S. Maekawa, *J. Phys. Soc. Jpn.* **75**, 034708 (2006).
- ³³ S. Ideta *et al.*, *Phys. Rev. Lett.* **104**, 227001 (2010).
- ³⁴ Y. Chen *et al.*, *Phys. Rev. Lett.* **103**, 036403 (2009).
- ³⁵ M.-H. Julien, P. Carreta, M. Horvatić, C. Berthier, Y. Berthier, P. Ségransan, A. Carrington, and D. Colson, *Phys. Rev. Lett.* **76**, 4238 (1996).
- ³⁶ H. Kotegawa, Y. Tokunaga, K. Ishida, G.-q. Zheng, Y. Kitaoka, H. Kito, A. Iyo, K. Tokiwa, T. Watanabe, and H. Ihara, *Phys. Rev. B* **64**, 064515 (2001).
- ³⁷ D. H. Kim and P. A. Lee, *Ann. Phys.* **272**, 130 (1999).
- ³⁸ N. D. Mermin and H. Wagner, *Phys. Rev. Lett.* **17**, 1133 (1966).